Azerbaijan University of Architecture and Construction
ISSN 2706-7726

Engineering Mechanics
Scientific and Technical Journal

E-mail: engineeringmechanics@azmiu.edu.az

September 2022	Issue 12	Volume 4	Number 3	Pages 3-14

STABILITY OF PLATES AND SHELLS ON IMPACT

Ismail R. Sadigov
Azerbaijan University of Architecture and Construction, Baku.

Abstract *- The scope of tasks did not include the case of a very fast – shock – load application, since its study should be carried out taking into account the wave nature of the propagation of stresses in the shell or plate. Let us now turn to the case of shock loading of plates and shells. It should be noted that the theory of shock resistance of shells and plates can be used in the calculations of thin-walled structures for the effect of explosive and seismic loads. Reality often poses the task of calculating thin-walled structural elements taking into account special physical conditions, for example, radiation heating, radiation exposure, heat stroke, etc. All this puts forward the need for a special calculation of shells and plates. Some issues of this kind are covered in the provided article, namely: the formulation of the problem of determining the bearing capacity of shells and plates; the problem of calculating the strength of shells subjected to radiation heating or exposed to radiation, heat stroke and the theory of thermal boundary layer. The bearing capacity of the shell and plates is the limiting value of the external forces at which the internal forces T and moments M satisfy the final ratio [2], the equilibrium equations, the conditions of compatibility of deformations and boundary conditions. In some special cases, due to the finite relation, the equilibrium problem becomes statically definable and does not require conditions for the compatibility of deformations. Then the question of the bearing capacity of the shell and plates is solved relatively simply. It is even more simplified if forces and moments can be expressed in terms of external forces only using equilibrium equations, which is the case, for example, in the momentless theory of shells and plates; in this case, the final ratio [3] determines the bearing capacity in which this article is considered.*

Keywords: *shock application, wave character, inertia forces, deflections from shifts, moment of time, symmetrical impact, dynamic stability, inertial stresses, axial compression, dent belts, time parameters, weight of the striking body, of course large, striking mass, double-humped curve, impact velocity, wave formation, impact effect, shapes dents.*

1. INTRODUCTION

We will compose new initial equations, assuming that the deflections during buckling of the shell can be comparable to its thickness; in addition, we will take into account the initial deviations of the shape of the median surface from the ideal one. We refer the coordinate lines to the main directions and denote the main curvatures of the median surface by $\kappa_x$and κ_y.

Expressions for deformations in the median surface have the form according to (12.120) (for shear deformation, the designation γ is introduced here, since the specific gravity of the material is further understood by γ):

$$\left.\begin{aligned} \varepsilon_x &= \frac{\partial u}{\partial x} - \kappa_x(w - w_0) + \frac{1}{2}\left(\frac{\partial w}{\partial x}\right)^2 - \frac{1}{2}\left(\frac{\partial w_0}{\partial x}\right)^2, \\ \varepsilon_y &= \frac{\partial v}{\partial y} - \kappa_y(w - w_0) + \frac{1}{2}\left(\frac{\partial w}{\partial y}\right)^2 - \frac{1}{2}\left(\frac{\partial w_0}{\partial y}\right)^2, \\ \bar{\gamma} &\frac{\partial u}{\partial y} + \frac{\partial v}{\partial y} + \frac{\partial w}{\partial x}\frac{\partial w}{\partial y} - \frac{\partial w_0}{\partial x}\cdot\frac{\partial w_0}{\partial y}. \end{aligned}\right\} \tag{1}$$

The equation of compatibility of deformations by analogy with (12.110) is written as

$$\frac{\partial^2 \varepsilon_x}{\partial y^2} + \frac{\partial^2 \varepsilon_y}{\partial x^2} - \frac{\partial^2 \bar{\gamma}}{\partial x \partial y} = \frac{1}{2}[L(w, w) - L(w_0, w_0)] - \nabla_k^2(w - w_0) \tag{2}$$

$L(w, w)$ and $\nabla_k^2\, w$ are understood as expressions

$$\left.\begin{aligned} L(w, w) &= 2\left[\frac{\partial^2 w}{\partial x^2} + \frac{\partial^2 w}{\partial y^2} - \left(\frac{\partial^2 w}{\partial x \partial y}\right)^2\right], \\ \nabla_k^2 &= \kappa_y \frac{\partial^2 w}{\partial x^2} + \kappa_x \frac{\partial^2 w}{\partial y^2}. \end{aligned}\right\}$$

Next, we write out the equations of motion of the shell element with the addition of inertia forces corresponding to the displacements and, v along the coordinate lines. The equations of motion in projections on tangents to the lines x, y will be:

$$\left.\begin{aligned} \frac{\partial \sigma_x}{\partial x} + \frac{\partial \tau}{\partial y} - \frac{\gamma}{g}\frac{\partial^2 u}{\partial t^2} &= 0, \\ \frac{\partial \tau}{\partial x} + \frac{\partial \sigma_y}{\partial y} - \frac{\gamma}{g}\frac{\partial^2}{\partial t^2} &= 0. \end{aligned}\right\} \tag{3}$$

and the equation in projections on the normal to the median surface

$$\begin{aligned} \frac{D}{h}\nabla^4(w_0, w_0) &= \sigma_x\kappa_x + \sigma_y\kappa_y + \\ + \frac{\partial}{\partial x}\left(\sigma_x\frac{\partial w}{\partial x} + \tau\frac{\partial w}{\partial y}\right) &+ \frac{\partial}{\partial y}\left(\tau\frac{\partial w}{\partial x} + \sigma_y\frac{\partial w}{\partial y}\right) - \frac{\gamma}{g}\frac{\partial^2 w}{\partial t^2} + \frac{q}{h} \end{aligned} \tag{4}$$

These equations do not include terms reflecting the inertia of rotation of the shell elements and deflections from shifts, based on the results obtained for rods in problems of this type, these terms can be neglected.

The relations between deformations and stresses will be:

$$\sigma_x = \frac{E}{1-\mu^2}\left(\varepsilon_x + \mu\varepsilon_y\right), \quad \sigma_y = \frac{E}{1-\mu^2}\left(\varepsilon_y + \mu\varepsilon_x\right), \quad \tau = \frac{E}{2(1+\mu)}\bar{\gamma}. \tag{5}$$

Ninth equations (1), (3) – (5), corresponding to nine unknown displacements, deformations and stresses with the addition of boundary and initial conditions, allow, generally speaking, to solve the problem. However, in some cases, for example, for closed cylindrical or conical shells, this scheme turns out to be too complicated; it is desirable to look for ways to simplify it.

One of the options for this simplification is as follows. We introduce expressions (5) and (1) into the first equation (3), then we get,

$$\begin{gathered}\frac{\gamma}{g}\frac{\partial^2 u}{\partial t^2} = \frac{E}{1-\mu^2}\left(\frac{\partial}{\partial x}\left\{\frac{\partial u}{\partial x} - \kappa_x(w - w_0) + \frac{1}{2}\left(\frac{\partial w}{\partial x}\right)^2 - \frac{1}{2}\left(\frac{\partial w_0}{\partial x}\right)^2 + \right.\right. \\ \left. +\mu\left[\frac{\partial v}{\partial y} - \kappa_y(w - w_0) + \frac{1}{2}\left(\frac{\partial w}{\partial y}\right)^2 - \frac{1}{2}\left(\frac{\partial w_0}{\partial y}\right)^2\right]\right\} + \\ \left. + \frac{1}{2}(1-\mu)\frac{\partial}{\partial y}\left[\frac{\partial u}{\partial y} + \frac{\partial v}{\partial x} + \frac{\partial w}{\partial x}\frac{\partial w}{\partial y} - \frac{\partial w_0}{\partial x}\frac{\partial w_0}{\partial y}\right]\right)\end{gathered} \tag{6}$$

Let us take into account that the process of buckling of the shell upon impact can be conditionally divided into two stages: the first consists mainly in the accumulation of stresses in the median surface, the second, in the sharp buckling of the shell and the development of significant deflections. When considering the first stage, it is possible, apparently, to neglect the effect of deflection on the inertia forces in the median surface, the second, a sharp bulging of the shell and the development of significant deflections. When considering the first stage, it is possible, apparently, to neglect the effect of deflection on the inertia forces in the median surface. As for the second stage, here the "contribution" of the deflections of the shell to the total value of the tangential inertia forces may be noticeable; but at the same time, the influence of the inertia forces themselves in the median surface on the behavior of the shell should not be significant. Proceeding from this, we agree to neglect the deflection effect when determining the inertia forces in the median surface and for the entire buckling process of the shell.
And so, instead of expressions of type (6), we take the following relations:

$$\left.\begin{aligned}\frac{\gamma}{g}\frac{\partial^2 u}{\partial t^2} &= \frac{E}{1-\mu^2}\left[\frac{\partial^2 u}{\partial x^2} + \mu\frac{\partial^2 v}{\partial x \partial y} + \frac{1}{2}(1-\mu)\left(\frac{\partial^2 u}{\partial y^2} + \frac{\partial^2 v}{\partial x \partial y}\right)\right]; \\ \frac{\gamma}{g}\frac{\partial^2 v}{\partial t^2} &= \frac{E}{1-\mu^2}\left[\frac{\partial^2 v}{\partial y^2} + \mu\frac{\partial^2 u}{\partial x \partial y} + \frac{1}{2}(1-\mu)\left(\frac{\partial^2 v}{\partial x^2} + \frac{\partial^2 u}{\partial x \partial y}\right)\right].\end{aligned}\right\} \tag{7}$$

Equations (7) together with the initial and boundary conditions allow us to determine the displacements and, *v*. These equations are used in the study of the propagation of elastic waves in the median surface of the shell. Knowing the functions *u; v*, we find the stresses in the median surface. Then you can go to equation (4), with which the deflection function *w* is found.

Another way is to introduce a dynamic stress function in the median surface. Differentiating the first and second equations (3) by x and y, respectively, we obtain:

$$\left.\begin{aligned}\frac{\partial^2\sigma_x}{\partial x^2}+\frac{\partial^2\tau}{\partial x\partial y}-\frac{\gamma}{g}\frac{\partial^3 u}{\partial x\partial t^2}=0,\\ \frac{\partial^2\tau}{\partial x\partial y}+\frac{\partial^2\sigma_y}{\partial y^2}-\frac{\gamma}{g}\frac{\partial^2 v}{\partial y\partial t^2}=0,\end{aligned}\right\} \tag{8}$$

We further define the derivatives of *u* and *v* included in (8) from the relation (1), omitting the terms depending on the deflection of *w* according to the above condition, we find:

$$\frac{\partial^3 u}{\partial x\partial t^2}\approx\frac{\partial^2\varepsilon_x}{\partial t^2},\;\; \frac{\partial^3 v}{\partial y\partial t^2}\approx\frac{\partial^2\varepsilon_y}{\partial t^2} \tag{9}$$

Using (8) and (5), we will have taking into account (9):

$$\left.\begin{aligned}\frac{\partial^2\sigma_x}{\partial x^2}+\frac{\partial^2\tau}{\partial x\partial y}-\frac{\gamma}{Eg}\left(\frac{\partial^2\sigma_x}{\partial t^2}-\mu\frac{\partial^2\sigma_y}{\partial t^2}\right)=0,\\ \frac{\partial^2\tau}{\partial x\partial y}+\frac{\partial^2\sigma_y}{\partial y^2}-\frac{\gamma}{Eg}\left(\frac{\partial^2\sigma_y}{\partial t^2}-\mu\frac{\partial^2\sigma_x}{\partial t^2}\right)=0,\end{aligned}\right\} \tag{10}$$

We express σ_x and σ_y in terms of the stress function ϕ by formulas generalizing the known formulas (13.13) to the dynamic case:

$$\left.\begin{aligned}\sigma_x=\frac{\partial^2\phi}{\partial y^2}-\frac{\gamma}{Eg}(1+\mu)\frac{\partial^2\phi}{\partial t^2},\\ \sigma_y=\frac{\partial^2\phi}{\partial x^2}-\frac{\gamma}{Eg}(1+\mu)\frac{\partial^2\phi}{\partial t^2}.\end{aligned}\right\} \tag{11}$$

Each of the equations (10) will then lead to the following equation relating the tangential stressτ_c by the function ϕ:

$$\frac{\partial^2\tau}{\partial x\partial y}=-\frac{\partial^4\phi}{\partial x^2\partial y^2}+\frac{\gamma}{Eg}\frac{\partial^2}{\partial t^2}\nabla^2\phi-\left(\frac{\gamma}{Eg}\right)^2(1-\mu^2)\frac{\partial^4\phi}{\partial t^4} \tag{12}$$

Substituting (11) into the equation of motion (4), we bring it to the form

$$\frac{D}{h}\nabla^4(w - w_0) = L(\phi, w) + 2\tau\frac{\partial^2 w}{\partial x \partial y} + \nabla_k^2\phi - \\ -\frac{\gamma}{Eg}(1+\mu)\left(k_x + k_y + \nabla^2 w\right)\frac{\partial^2\phi}{\partial t^4} - \frac{\gamma}{g}\frac{\partial^2 u}{\partial t^2} + \frac{q}{h}, \tag{13}$$

where

$$\frac{\partial^2\sigma_x}{\partial y^2} - 2\frac{\partial^2\tau}{\partial x\partial y} + \frac{\partial^2\sigma_y}{\partial x^2} - \mu\left(\frac{\partial^2\sigma_x}{\partial x^2} + 2\frac{\partial^2\tau}{\partial x\partial y} + \frac{\partial^2\sigma_y}{\partial y^2}\right) = \\ = E\left\{-\frac{1}{2}[L(w,w) - L(w_0,w_0)] - \nabla_k^2(w - w_0)\right\} \tag{14}$$

Using (8) and (9), we get

$$\frac{1}{E}\left[\nabla^2 - \frac{\gamma}{Eg}(1-\mu^2)\frac{\partial^2}{\partial t^2}\right]\left[\nabla^2 - \frac{2\gamma}{Eg}(1+\mu)\frac{\partial^2}{\partial t^2}\right]\phi = \\ = -\frac{1}{2}[L(w,w) - L(w_0,w_0)] - \nabla_k^2(w - w_0) \tag{15}$$

System of equations (13), (15), (12) with respect to the functions ϕ, w and τ, it is final; it must be supplemented by boundary and initial conditions*).In the special case of the static problem (13) and (15) pass into the usual system of equations of nonlinear shell theory.
Discarding the nonlinear terms in (13) and (15) and counting $w_0 \equiv 0$, we come to the following basic equations of dynamic linear theory:

$$\left.\begin{aligned} \frac{D}{h}\nabla^4 w = \nabla_k\phi\frac{\gamma}{Eg}(1+\mu)\left(k_x + k_y\right)\frac{\partial^2\phi}{\partial t^2} - \frac{\gamma}{g}\frac{\partial^2 u}{\partial t^2} + \frac{q}{h}; \\ \frac{1}{E}\left[\nabla^2 - \frac{\gamma}{Eg}(1-\mu^2)\frac{\partial^2}{\partial t^2}\right]\left[\nabla^2 - \frac{2\gamma}{E}(1+\mu)\frac{\partial^2}{\partial t^2}\right]\phi = -\nabla_k^2 w \end{aligned}\right\} \tag{16}$$

In some problems, it is possible to approximately put $\tau \equiv 0$; then the system (13) – (15) will be reduced to two simpler equations. The solution of the system (13) – (15) can be carried out using digital machines; in this case, the finite difference method can be used.

2. PLATE AND CYLINDRICAL PANEL AT LONGITUDINAL IMPACT

We investigate the behavior of a plate or a cylindrical circular panel that perceives the impact of a rigid mass in the direction of one of the sides of the plate or along the forming shell. We assume that the forces transmitted by the striking mass are evenly distributed along one of the transverse edges and that the second transverse edge is stationary (Fig. 22.1).

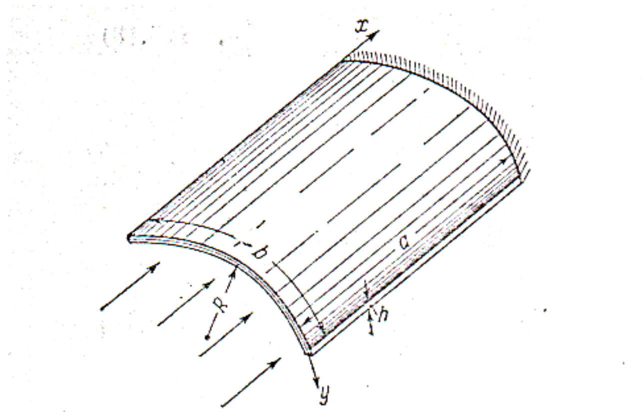

Fig. 22.1. Cylindrical panel under the action of axial impact.

3. VARIOUS APPROACHES TO THE APPROXIMATE SOLUTION OF THE PROBLEM. HIGHLIGHTING THE NARROW ZONE OF THE SHELL

Integrating the above equations is a difficult task, even with the use of the most powerful of modern digital machines. Therefore, it is desirable to find some other ways of research that allow using the already developed methods of the theory of dynamic stability of shells *). It is possible, for example, for each moment of time to average the "inertial stresses" found from equations (7) in the median surface, either along the entire length of the shell, or along some narrow zone covering part of the length.

Consider here the second of these techniques, already used earlier. We select some cross-sections of the shell and determine the law of change of compressive inertial stresses, taking into account the successive reflections of the elastic wave from the ends. For an axisymmetric impact, we must take $v \equiv 0$ in (7) and then instead of (15) we get the well-known "core" equation (8.2) with the replacement of E by $E/(1-\mu^2)$. Integrating this equation using, for example, the method of characteristics, or using equation (8.18a) in finite differences, we determine the law of variation of inertial compressive stresses P in time for different cross sections of the shell.

Further, we assume that the law of change of compressive stresses found extends to a narrow zone near the cross section. We compose dynamic equations of type (13) and (15), assuming that the inertial components have already been determined at the previous stage of calculations. Then instead of (15) we get the usual equation,

$$\frac{1}{E}\nabla^2\phi = \frac{1}{2}[L(w,w) - L(w_0,w_0)] - \nabla_k^2(w - w_0). \quad (17)$$

Assuming that the dents that occur during buckling of the shell have a diamond-shaped character, we accept expressions for complete and initial deflection, as usual, in the form:

$$\left.\begin{aligned} w &= f(\sin\alpha x \sin\beta y + \psi \sin^2\alpha x \sin^2\beta y), \\ w_0 &= f_0(\sin\alpha x \sin\beta y + \psi \sin^2\alpha x \sin^2\beta y). \end{aligned}\right\}, \quad (18)$$

or

$$\left.\begin{aligned} w &= f(sin\alpha x\, sin\beta y + \psi sin^2\alpha x), \\ w_0 &= f_0(sin\alpha x\, sin\beta y + \psi sin^2\alpha x). \end{aligned}\right\}, \tag{19}$$

where $\alpha = m\pi/L\,, \beta = n/R$. Substituting (18) or (19) into (17), we find the function ϕ; in the expression for ϕ we enter the term$(-py^2/2E)$, and $p = p(t)$ is determined for the selected zone of the shell, as mentioned above. By choosing expressions of type (18) or (19) for the deflection and finding the integral of equation (17), we obtain not well-defined boundary conditions for the edges of the zone under consideration. Such boundary conditions are usually assumed with respect to the ends of the shell when considering a static nonlinear problem in the case of axial compression. These conditions in the linearized problem correspond to the case of hinged fastening of the shell with translationally shifting flat ends. Some justification for the proposed procedure is the assumption that the shell length zone is selected, although it is narrow, but still covers several belts of dents; then the boundary conditions should not greatly affect the results of calculations.

So, we consider the law of time variation of functions ϕ to be established. Further calculations are reduced to using the Bubnov–Galerkin method with respect to an equation of type (13); this procedure is described in detail above. In the process of solving the problem, the parameters ψ, ξ=α/β and n should be selected. The first of them, which determines the dependence between the symmetric and non-symmetric parts of the deflection, can be chosen the same as in the static problem; carried out according to a more complex scheme showed that such an assumption is acceptable. As for the parameter ξ, it determines the shape of the dent and is equal to the ratio of the size of the dent along the arcs s_y to the size of the generatrix s_x. N refers to the number of dents along the cross section. These values change dramatically depending on the circumstances of dynamic loading.

For example, Figure 22.5 shows the dependences obtained using a digital machine between the deflection boom parameter ζ and the time parameter t* for the case when a shell with a radius-to-thickness ratio$R/h = 180$ is struck by an infinitely large mass $(Q_1/Q_2 \to \infty)$ with a speed of $V_0 = 0{,}001\, c$. The diagrams refer to the zone of the shell adjacent to the end face on which the impact is made. It is assumed that the amplitude of the initial deflection $\zeta_0 = f_0/h$ is 0.001 of the thickness of the shell. All curves have three sections: the first, which characterizes the initial stage of buckling and almost merges with the abscissa axis (it is not shown in the figure), the second, which describes the transitional stage of rapid growth of the deflection, i.e., the process of the shell actually snapping, and the third section, which characterizes the nonlinear oscillations of the shell after snapping. The curves of Fig. 22.5 are constructed for the case ξ=2. As you can see, the rapid growth front of deflections occurs first of all for the diagram that corresponds to the number of waves n = 11; the transition sections of curves n = 10 and n =12 lie to the right. This problem is a continuation of the problem we considered earlier about the stability of the rod under axial impact *). Let's use the relations between deformations and displacements, the equilibrium equations and the relations of Hooke's law. Then we will get nine equations regarding displacements, deformations and stresses as functions of spatial coordinates *x, y* and time *t*. In order to lower the order of equation (4), it is advisable to introduce a new function $\omega = \nabla^2(w - w_0)$, then in (4), the function $\nabla^2 w$ will appear.

Let's choose the following initial conditions: $w = w_0$, $u = v = 0$, $\partial w/\partial t = \partial u/\partial t = \partial v/\partial t = 0$ by $t = 0$.The boundary conditions take $w = 0$, $\partial^2 w/\partial n^2 = 0$, $\tau = 0$ for all the contour points ($\partial^2 w/\partial n^2$ − norms of the derivative along the contour), $(Q_1/8)\ \partial^2 u/\partial t^2 = hb\sigma_x$ when x=0, where $Q1-$ the weight of the striking body; u = 0 at x = 0, v = 0 at y = 0 and

y=b. The expressions for the initial deflection will be chosen in the form $w_0 = f_0 \sin(\pi x/a) \sin(\pi y/b)$.

The equations listed above, as well as the initial and boundary conditions, were reduced to a dimensionless form and expressed in finite differences. The solution of finite difference equations was performed on a BESM–2M machine with a step in spatial coordinates of 1/12 and 1/16 from side b. The time step was chosen from the stability condition of the difference scheme*).

Figure 22.2 shows the time variation of the compressive stress parameter$\bar{\sigma}_x = \sigma_x b^2/Eh^2$ along the line $y = b/2$ for the case of a square plate (on the left is the end being impacted). The ratiot/T is denoted by $t*$, where T is the time of passage of longitudinal elastic waves along the side a. The removing mass is considered infinitely large here; the arrow of the initial loss is 0.001 of the thickness h of the plate.

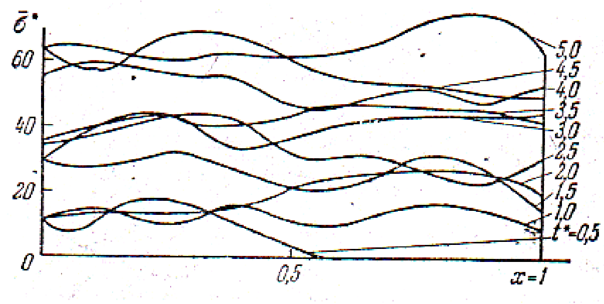

Fig. 22.2. Change of compressive stresses in the middle section of the plate over time.

Fig. 22.3 for the same example, the values of the additional dimensionless deflection w/h along the line $y = b/2$ (solid curves) and the line $x = a/2$ (dotted line) are given at successive times; the curved surface is symmetrical with respect to $y = b/2$. As you can see, with the selected impact velocity in both directions, one half-wave of a peculiar shape is formed, which later transforms into a two-humped curve.

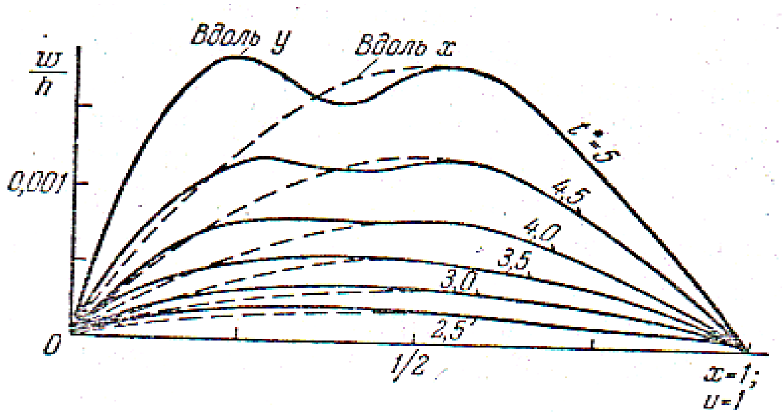

Fig. 22.3. Distribution of deflections in different sections of the plate upon impact.

Figure 22.4 refers to a cylindrical panel with the parameter $b^2/Rh = 48$; the figure shows the curved surface of the panel of several reflections of the compression wave from the ends. Along the contour of the panel, a fold is formed in the direction from the center of curvature, and in the middle part, there is a deep dent facing the center. Obviously, at the moment of time to which the drawing refers, the process of preliminary wave formation is completed, after which the panel should be clicked. We conclude from this that the most probable in this example is the buckling of the shell with the number of waves n = 11.

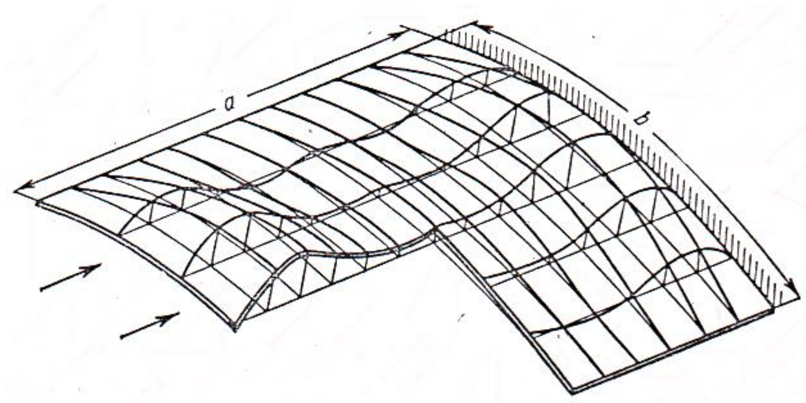

Fig. 22.4. Deflection distribution in the case of a cylindrical panel upon impact.

Results similar to those shown in Fig. 22.5 were obtained for other shell sections. As expected, this result applies only to shells of accepted sizes, when the buckling process covers a significant number of elastic wave reflections from both ends of the shell.

Calculations have shown that an increase in the impact velocity v_0 leads to an increase in the number of dents n, i.e. to the appearance of higher forms of loss of stability. At the same time, the critical value of the load parameter also increases. Comparison of the "deflection – time" diagrams allows you to determine the impact effect. From the comparison of the dynamic and static diagram, it is possible to judge whether the impact will lead to the cracking of the shell, which is the main purpose of the study.

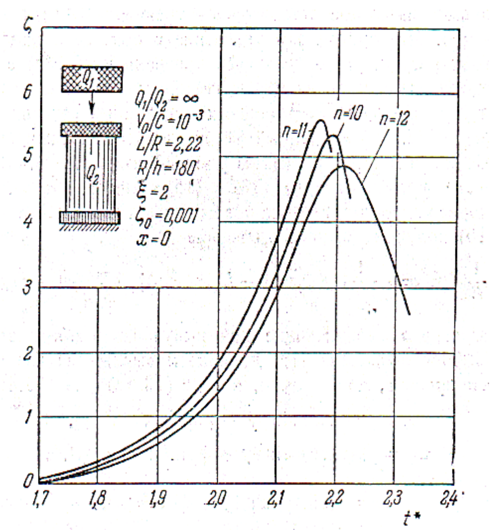

Fig. 22.5. The dependence of the deflection boom on time with a different number of waves.

The results of calculations related to the change in the shape of the dent depending on the impact parameters are interesting. With an infinitely large impacting mas$(Q_2/Q_1 \longrightarrow 0)$s, the dents are strongly elongated along the arc, so that the value of $\xi = S_y/S_x$ is about 4 (Fig. 22.6).If the ratio of the weight of the load to the weight of the shell is 5, then the dents turn out to be almost square (ξ≈1).

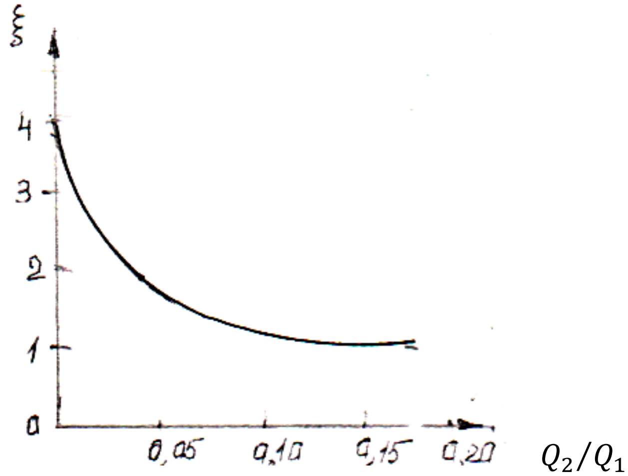

Fig. 22.6. The nature of the dents on impact, depending on the ratio between the weights of the load and the shell.

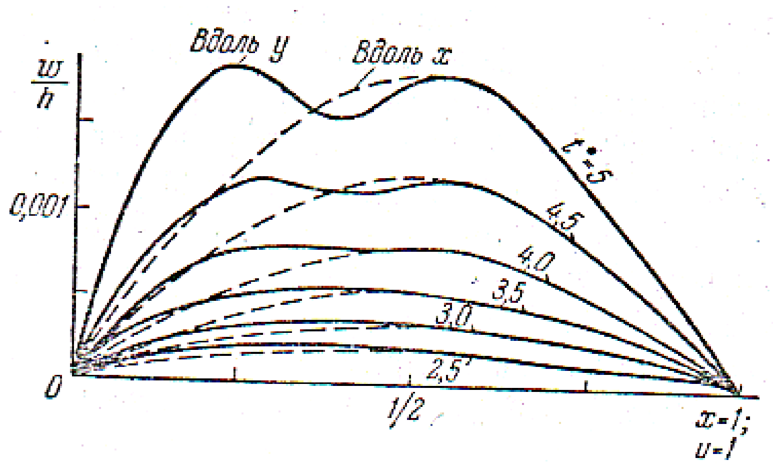

Fig. 22.3. Distribution of deflections in different sections of the plate upon impact.

Figure 22.4 refers to a cylindrical panel with the parameter $b^2/Rh = 48$; the figure shows the curved surface of the panel of several reflections of the compression wave from the ends. Along the contour of the panel, a fold is formed in the direction from the center of curvature, and in the middle part, there is a deep dent facing the center. Obviously, at the moment of time to which the drawing refers, the process of preliminary wave formation is completed, after which the panel should be clicked. We conclude from this that the most probable in this example is the buckling of the shell with the number of waves n = 11.

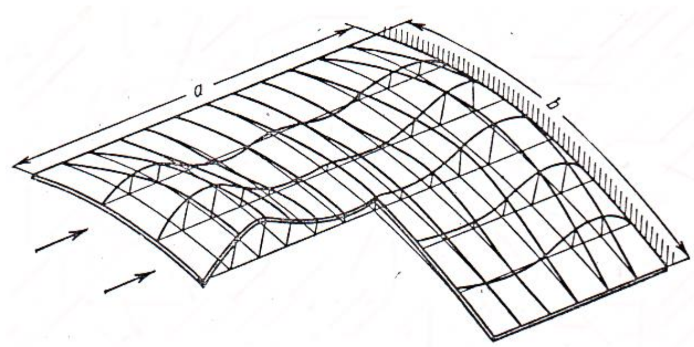

Fig. 22.4. Deflection distribution in the case of a cylindrical panel upon impact.

Results similar to those shown in Fig. 22.5 were obtained for other shell sections. As expected, this result applies only to shells of accepted sizes, when the buckling process covers a significant number of elastic wave reflections from both ends of the shell.

Calculations have shown that an increase in the impact velocity v_0 leads to an increase in the number of dents n, i.e. to the appearance of higher forms of loss of stability. At the same time, the critical value of the load parameter also increases. Comparison of the "deflection – time" diagrams allows you to determine the impact effect. From the comparison of the dynamic and static diagram, it is possible to judge whether the impact will lead to the cracking of the shell, which is the main purpose of the study.

4. EXPERIMENTAL DATA

Let us consider the results of a series of experiments in which the behavior of duralumin cylindrical shells under axial impact was determined. The scheme of the experimental setup is shown in Fig. 22.7. The sample was subjected to impact was ensured by the fact that the load moved along the cable, which was given a known tension.

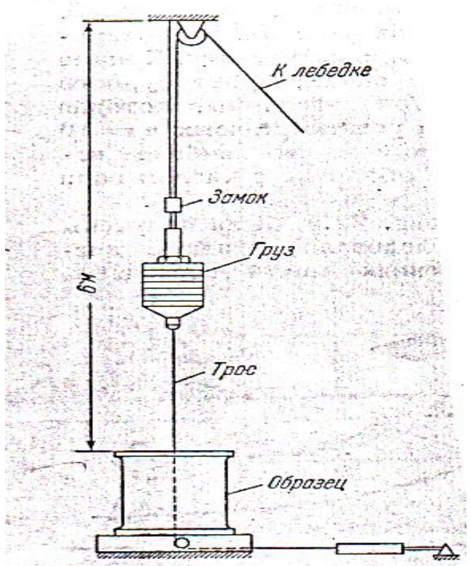

Fig. 22.7. Installation for testing shells for longitudinal impact.

The study of the process of time variation of deformations and stresses in various sections of the shell was carried out using wire strain gauges, the signals from which were recorded by a two-beam cathode oscilloscope. The readings recorded on the oscilloscope screen were photographed. When testing some samples, an eight-loop oscilloscope was used to measure deformations.

Wire sensors were glued in different sections from the outer and inner sides of the shell; this made it possible to isolate the stresses in the median surface and the stresses of the actual bending. The entire impact process, judging by the timestamps, took about 1100 microseconds. After recalculation, it turned out that the maximum stresses in the $x=L$ section were about 3000 kg / sm2 (after 740 microseconds), and in the x= L⁄2 section, and in the $x=L/2$ section - about 1900 kg / sm2 (after 700 microseconds).

In the experiments carried out, dents were located, as a rule, at the end of the shell experiencing an impact and at the stationary end, forming one or two belts in each of these zones.

Figure 22.12 shows a comparison of experimental data of critical stresses with theoretical results. The curve in the figure shows the dependence of the dynamic critical voltage parameter (related to the upper static voltage parameter P_b^*) on the ratio of the shell mass to the weight of the load. This diagram corresponds to the results of calculations according to the procedure described earlier. The circles here indicate the experimental values of stresses determined from experiments at $R/h = 180$. The impact velocity parameter was equal to $v_0/c = 10^{-3}$, where v_0 is the initial impact velocity, c is the velocity of propagation of longitudinal elastic waves in the shell material.It can be seen from Figure 22.12 that all experimental points are located close enough to the theoretical curve and at the same time from above it.

5. REFERENCES

1. Agamirov V.L., Volmir A.S. On the stability of a cylindrical shell under longitudinal impact. DAN USSR 157, No. 2, 1964. Investigation of the stability of cylindrical shells under longitudinal impact. Problems of stability in structural mechanics. Gosstroyizdat, M., 1965.

2. Agamirov V.L., Smetanina L.N. Experimental studies of the stability of cylindrical shells under longitudinal impact. Abstracts of the 5th All–Union Conference on the Theory of Plates and Shells, Moscow, 1965.

3. Borisenko V.I. On the stability of a cylindrical shell under longitudinal impact. Applied mechanics 10, №6, 1964; №5, 1965, 100 – 104; 1, №8, 1965, 57 – 62; " Problems of stability in construction mechanics", Gosstroyizdat. M., 1965.

4. Volmir A.S. Impact stability. Abstracts of reports of the 5th All–Union Conference on the Theory of Plates and Shells, Moscow, 1965; Collection of articles dedicated to I.M. Rabinovich, Gosstroizdat, 1966.

5. Volmir A.S., Kildibekov I.G. To the study of the behavior of shells and plates on impact. Izv. Universities. Mechanical Engineering, No. 7, 1964.

6. Protsenko O.P. Dynamic stability of a cylindrical shell with an initial loss under the combined action of axial compression and external pressure, cand. diss., Kiev, 1965.

7. Yangurazov Sh.Kh. Dynamic stability of a pivotally supported cylindrical shell with an initial one under longitudinal impact. Sat. scientific research. works of the Tashkent text. In – ta 14, 1962.